Chemical Science

ROYAL SOCIETY OF CHEMISTRY

EDGE ARTICLE

View Article Online
View Journal | View Issue

Check for updates

Cite this: *Chem. Sci.*, 2022, **13**, 9232

All publication charges for this article have been paid for by the Royal Society of Chemistry

Received 5th May 2022
Accepted 12th July 2022

DOI: 10.1039/d2sc02530b

rsc.li/chemical-science

Cation assisted binding and cleavage of dinitrogen by uranium complexes†

Nadir Jori, [a] Thayalan Rajeshkumar,[c] Rosario Scopelliti, [a] Ivica Živković, [b] Andrzej Sienkiewicz, [de] Laurent Maron[c] and Marinella Mazzanti *[a]

The role of alkali promoters in N_2 cleavage by metal complexes remains poorly understood despite its relevance to the industrial production of ammonia from N_2. Here we report a series of alkali bound-oxo-bridged diuranium(III) complexes that provide a unique example of decreasing N_2 binding affinity with increasing cation size (from K to Cs). N_2 binding was found to be irreversible in the presence of K. A N_2 complex could be isolated in the solid state in the presence of the Rb cation and crystallographically characterized, but N_2 binding was found to be reversible under vacuum. In the presence of the Cs cation N_2 binding could not be detected at 1 atm. Electrochemical and Computational studies suggest that the decrease in N_2 binding affinity is due to steric rather than electronic effects. We also find that weak N_2 binding in ambient conditions does not prevent alkali assisted N_2 cleavage to nitride from occurring. More importantly, we present the first example of cesium assisted N_2 cleavage leading to the isolation of a N_2 derived multimetallic U/Cs bis-nitride. The nitrides readily react with protons and CO to yield ammonia, cyanate and cyanide.

Introduction

Uranium compounds are attracting increasing interest in catalysis and in the activation of small molecules such as N_2 and CO_2.[1] Inorganic uranium compounds were also reported in early studies to be efficient catalysts for N_2 conversion to ammonia,[2] but iron-based catalysts were adopted in the Haber–Bosch process. As a result, the dinitrogen chemistry of molecular uranium compounds remains less developed[1j,m,3] than d-block metals, and only three examples of dinitrogen cleavage were reported so far (complexes **A–C** in Chart 1) where multimetallic cooperativity between uranium and s- or d-block metals is thought to play an important role.[4]

The role of multimetallic cooperativity and of alkali ions in dinitrogen binding and cleavage by mono- and multimetallic complexes has attracted large attention[1j,3j,5] due to its relevance to the iron-catalysed Haber–Bosch process for the industrial production of ammonia. Most catalysts developed for N_2 reduction to ammonia use potassium as an electronic promoter because it has showed higher efficiency than the other alkali ions.[5g,6] However, the role of alkali ions in dinitrogen cleavage remains poorly understood as most studies have focused on investigating the effects of N_2-bound alkali ions on the extent of dinitrogen activation in molecular dinitrogen complexes of transition metals[5g,7a,b] with rare examples of studies involving f elements being reported.[8,9] Fewer studies were directed to investigate the effect of alkali cations on N_2 binding affinity or N_2 cleavage and they were mostly limited to d-block metals and iron in particular.[5c,e,j,10] Examples of cation assisted dinitrogen

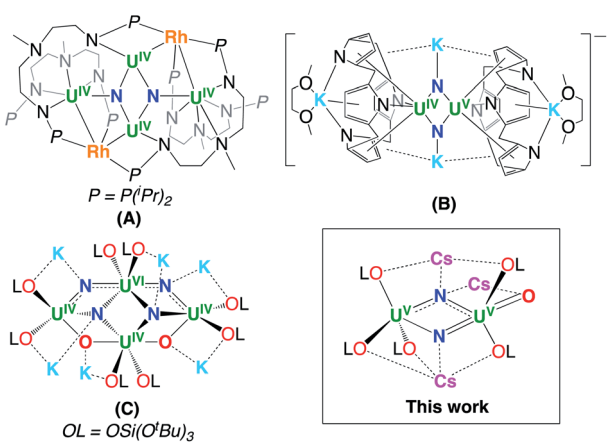

Chart 1 The eamples of dinitrogen cleavage by uranium complexes.

[a]*Insititut des Sciences et Ingénierie Chimiques, Ecole Polytechnique Fédérale de Lausanne (EPFL), 1015 Lausanne, Switzerland. E-mail: marinella.mazzanti@epfl.ch*

[b]*Laboratory for Quantum Magnetism, Institute of Physics, Ecole Polytechnique Fédérale de Lausanne (EPFL), Lausanne, 1015, Switzerland*

[c]*Laboratoire de Physique et Chimie des Nano-objets, Institut National des Sciences Appliquées, Cedex 4, 31077 Toulouse, France*

[d]*Laboratory for Quantum Magnetism, Institute of Physics, École Polytechnique Fédérale de Lausanne (EPFL), 1015 Lausanne, Switzerland*

[e]*ADSresonances Sàrl, Route de Genève 60B, 1028 Préverenges, Switzerland*

† Electronic supplementary information (ESI) available. CCDC 2154518–2154525. For ESI and crystallographic data in CIF or other electronic format see https://doi.org/10.1039/d2sc02530b

cleavage by d-block transition metals were reported for Li, Na K and Rb.[10b–d] In contrast, no example of dinitrogen cleavage promoted by Cs has been reported despite its higher reducing power. The role of the nature of the reducing alkali ions in the dinitrogen reduction has been investigated[5f,g,11] for molecular multimetallic complexes of iron but cleavage of N_2 was never observed in the presence of cesium most likely due to kinetic effects favouring the formation of multimetallic intermediates unable to promote N_2 cleavage.[5c,e,f,11a]

The few multimetallic uranium–alkali ion systems reported so far that effect the four-electron reduction of N_2,[1j,m,3h] or even its complete cleavage to nitride,[4] all contain the potassium cation. It should be noted that although the number of reported uranium nitride complexes is rapidly increasing[12,13] only three examples of uranium nitrides have been obtained from N_2 reduction (Chart 1).

Here we report the first example of cesium assisted N_2 cleavage which is effected by a multimetallic uranium–cesium complex. Moreover, we isolated a series of multimetallic complexes that are analogues of the previously reported oxide bridged diuranium(III)–K complex $[K_2\{U^{III}(OSi(O^tBu)_3)_3\}_2(\mu\text{-}O)]$[3h] presenting different alkali ions and demonstrated the important effects of the nature of the alkali ion on dinitrogen binding affinity and cleavage.

Results and discussion

U(III)/U(III) oxide-bridged complexes with different alkali metal counterions

We recently reported[3h] the well-defined multimetallic oxide bridged diuranium(III)–K complex $[K_2\{U^{III}(OSi(O^tBu)_3)_3\}_2(\mu\text{-}O)]$ **K_2-2** that effects the four-electron reduction of dinitrogen to yield the diuranium(V) complex $[K_2\{U^{V}(OSi(O^tBu)_3)_3\}_2(\mu\text{-}O)(\mu\text{-}N_2)]$, **$K_2$-$N_2$** which was further reduced by excess KC_8 to yield a multimetallic nitride cluster (**C**, Scheme 1) *via* a putative bis-nitride intermediate ("**K_4-$(N)_2$**") that could not be structurally characterized.[4c]

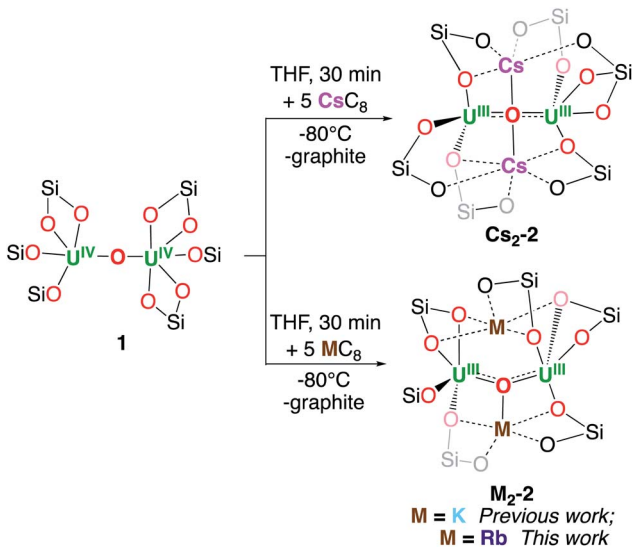

Scheme 1 Synthesis of M_2-2.

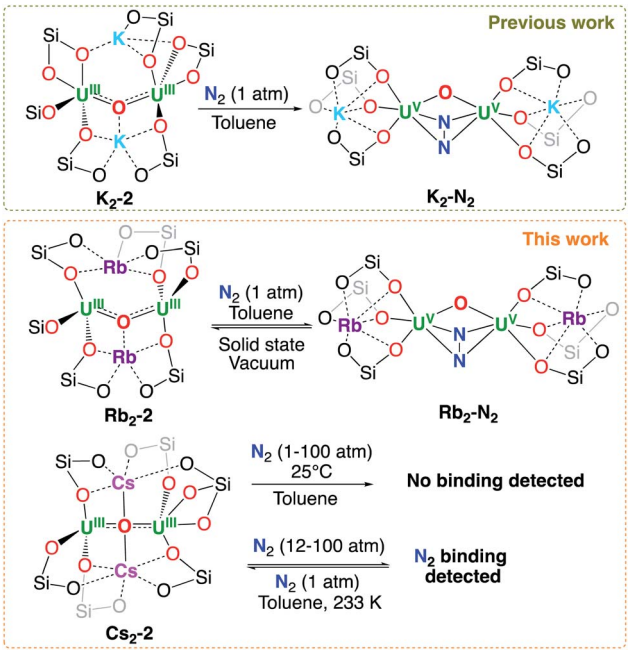

Scheme 2 N_2 reactivity of M_2-2.

Since **K_2-2** was obtained by reduction with KC_8 of the diuranium(IV) complex $[\{U^{IV}(OSi(O^tBu)_3)_3\}_2(\mu\text{-}O)]$, **1**, this system was identified as an ideal candidate to investigate the effect of the nature of alkali ions on dinitrogen cleavage by uranium complexes. Gratifyingly, the analogous dinuclear uranium(III) complexes $[M_2\{U^{III}(OSi(O^tBu)_3)_3\}_2(\mu\text{-}O)]$, (M = Rb, **$Rb_2$-2**; M = Cs, **$Cs_2$-2**), were obtained by reduction of complex **1** with 5 equivalents of RbC_8 or CsC_8 respectively in THF at −80 °C. The multimetallic U(III) complexes $[M_2\{U^{III}(OSi(O^tBu)_3)_3\}_2(\mu\text{-}O)]$, (M = Rb, Cs; **$Rb_2$-2** and **$Cs_2$-2**) (Scheme 1), were isolated from a cold (−40 °C) hexane and toluene solution with yields of 60 and 70% respectively.

The **M_2-2** complexes showed low thermal stability in THF solution, with a faster decomposition observed for **K_2-2** (complete decomposition over the course of 12 h)[3h] compared to **Rb_2-2** (60% remaining after 24 h) and **Cs_2-2** (80% remaining after 24 h). The stability of these complexes is greatly increased in THF solution at −40 °C, with 84% of **Cs_2-2** after 21 days and 62% of **Rb_2-2** after 14 days. Moreover, the complex **Cs_2-2** shows a remarkable stability in toluene solution at room temperature (no decomposition is observed up to 17 days), compared with **Rb_2-2** which decomposes completely over the course of 5 days and **K_2-2** which decomposes over the course of 24 h in the same conditions.[3h] The latter two decompose to a mixture of $[M_2\{U^{IV}(OSi(O^tBu)_3)_3\}_2(\mu\text{-}O)_2]$, **$M_2$-4** and other unidentified species. A few crystals of **Rb_2-4** could be isolated and characterized by X-ray diffraction (Fig. S59†) and ^{1}H NMR spectroscopy (Fig. S14†).

The synthesis of the Na and Li analogues was also pursued but, since the MC_8 reducing material is inaccessible, different synthetic strategies were followed without success. Notably, the reduction of **1** with Na^0 mirror led only to partial reduction and to the isolation of the mixed-valent complex [Na

$\{U^{III}(OSi(O^tBu)_3)_3\}\{U^{IV}(OSi(O^tBu)_3)_3\}(\mu\text{-}O)]$, **Na-3** in 30% yield (Fig. S58†).

The ^{1}H NMR spectra of $\mathbf{Rb_2}$**-2** and $\mathbf{Cs_2}$**-2** both show for the siloxide ligands a broad signal in THF at −40 °C and one sharp signal in toluene at −40 °C. Only one sharp signal is observed in the ^{1}H NMR spectra of $\mathbf{Rb_2}$**-2** and $\mathbf{Cs_2}$**-2** measured in toluene or THF at 25 °C suggesting fluxional behaviour in solution of the siloxide ligands. Similar ^{1}H NMR spectra have been reported for the $\mathbf{K_2}$**-2** complex. Overall, the binding of different cations results in a small shift of the signals assigned to the siloxide ligands (Fig. S15,† in a range of −0.08 ppm to −0.28 ppm in toluene solution at −40 °C). The sequential addition of 2 equiv. of 2.2.2-cryptand to a THF solution of $\mathbf{K_2}$**-2** at −40 °C, results in the displacement of the resonance assigned to the siloxide ligands (Fig. S58†). These studies indicate that the cations remain bound to the siloxides both in toluene and in THF solutions.

The solid-state molecular structure of $\mathbf{Rb_2}$**-2** (Fig. 1, middle) shows an ion-paired complex with two U(III) ions bridged by an oxo ligand, which also binds one Rb^+ cation (at a Rb–O distance of 3.007(6) Å) located in the pockets formed by four oxygen atoms of the siloxide ligands. A second Rb^+ cation is coordinated by five oxygen atoms of the siloxide ligands (2.899(6)–3.146(6) Å) but is located at a non-bonding Rb–O distance (3.696(6) Å).

The binding mode found in $\mathbf{Rb_2}$**-2** is similar to that reported for $\mathbf{K_2}$**-2** (Fig. 1, right) with an oxo bound K^+ at 2.913(4). Å and an unbound K^+ at 3.392(4) Å. The K^+ ions are bound by four and five siloxide oxygen atoms, respectively, at distances in the range 2.643(3)–3.008(4) Å, shorter than those found for the Rb-siloxides in $\mathbf{Rb_2}$**-2.**

The values of the U^{III}–(μ-O) distances (2.100(5) and 2.135(5) Å) are similar to those reported for **1** (2.085(1) and 2.137(1) Å) and compare well to the values reported for $\mathbf{K_2}$**-2**,[3h] and the only two other U(III) bridging oxo complexes previously reported.[14] The two uranium atoms are held in close proximity at a U–U distance of 4.1972(8) Å similar to that found in $\mathbf{K_2}$**-2** (4.262(1) Å). The U–(μ-O)–U core is bent (164.7(3)°), as was also reported for $\mathbf{K_2}$**-2** (167.4(2)°).

The solid-state molecular structure of $\mathbf{Cs_2}$**-2** (Fig. 1, left) displays a similar ion-paired dinuclear U(III) complex bridged by an oxo group at a U–U distance of 4.247(1) Å as $\mathbf{K_2}$**-2** and $\mathbf{Rb_2}$**-2**, but with some differences: first the binding of the oxo group to the U(III) centers in $\mathbf{Cs_2}$**-2** is more symmetric than in $\mathbf{K_2}$**-2** and in $\mathbf{Rb_2}$**-2** with two very similar U^{III}–(μ-O) distances (2.137(7) and 2.126(7) Å); second the U–(μ-O)–U core is almost linear (177.9(4)°) while it is bent in $\mathbf{K_2}$**-2** and in $\mathbf{Rb_2}$**-2.** Moreover, in $\mathbf{Cs_2}$**-2** both Cs^+ cations are coordinated to the oxo group (3.434(8) and 3.336(8) Å) (Table 1).

Overall, the binding of the cations K, Rb and Cs in the three complexes is quite similar, but we were interested in investigating how the observed structural differences would affect their magnetic properties and their reactivity.

Variable temperature SQUID magnetic data were measured for the complexes $\mathbf{Rb_2}$**-2** and $\mathbf{Cs_2}$**-2** and were compared with the previously reported magnetic data for $\mathbf{K_2}$**-2.**[3h] Data were measured only up to 250 K due to the low stability of the complexes above 250 K. The measured values of the magnetic moment per ion at 250 K are 2.1 μ_B for $\mathbf{K_2}$**-2,** 2.77 μ_B for $\mathbf{Rb_2}$**-2** and 2.51 μ_B for $\mathbf{Cs_2}$**-2** and decrease to a low value of 0.9 μ_B for $\mathbf{K_2}$**-2,** 0.7 μ_B for $\mathbf{Rb_2}$**-2** and 0.4 μ_B for $\mathbf{Cs_2}$**-2** at 2 K. Low values of χT at low temperature have been previously reported previously for other U(III) complexes.[15] The complex $\mathbf{Cs_2}$**-2** shows a significantly

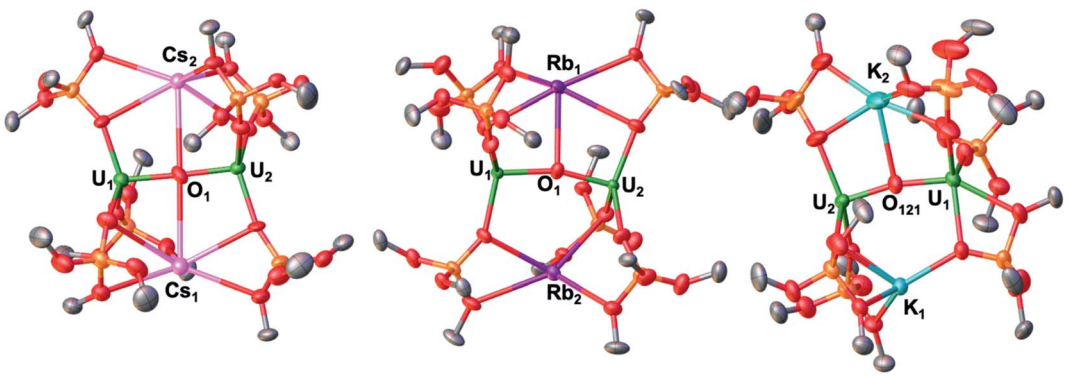

Fig. 1 Solid-state molecular structure of Cs_2-2 (left) Rb_2-2 (middle) and K_2-2 (redrawn from ref. 3h) with 50% probability ellipsoids. Color code: uranium (green), potassium (light blue) rubidium (purple), cesium (pink), oxygen (red), carbon (grey), silicon (orange). Hydrogen atoms and ^{t}Bu groups were omitted for clarity.

Table 1 Mean values of selected bond lengths (Å) and angles (°) in the complexes M_2-2

Complex	U–U	U1–(μ-O)	U2–(μ-O)	U1–(μ-O)–U2	M1–(μ-O)	M2–(μ-O)
$\mathbf{K_2}$**-2**	4.262(1)	2.178(3)	2.120(3)	167(4)	3.392(4)	2.913(4)
$\mathbf{Rb_2}$**-2**	4.1972(8)	2.135(5)	2.100(5)	164.7(3)	3.007(6)	3.696(6)
$\mathbf{Cs_2}$**-2**	4.247(1)	2.137(7)	2.126(7)	177.9(4)	3.336(8)	3.434(8)

different behaviour of the magnetic susceptibility measured in function of the temperature, as can be clearly observed in the plot of the magnetic susceptibility (χ) *versus* T (Fig. S65†). The χ *versus* T plot for **Cs_2-2** indicates the unambiguous presence of antiferromagnetic coupling between the U(III) centers, with a maximum of the χ at 10 K. In contrast, the plot of χ *versus* T of the **K_2-2** and **Rb_2-2** complexes shows the magnetic behaviour associated with two magnetically independent U(III) ions.[16] These results suggest that the presence of two Cs atoms in the core of the molecule allows a magnetic communication between the metal centers which is most likely correlated to a more covalent U–O–U bond in agreement with its linear geometry.

Binuclear complexes of uranium(III) are rare and only very few examples of magnetic communication between U(III) centers were reported including the diuranium(III) nitride complex $[K_3\{U^{III}(OSi(O^tBu)_3)_3\}_2(\mu\text{-}N)]$, **$K_3$UNU** complex[1j] which showed antiferromagnetic coupling with a maximum at a T of 23 K.[3h] Stronger antiferromagnetic coupling with the highest value of χ at 110 K was reported by Cummins and Diaconescu for an arene-bridged U(III) dimer.[15a,17]

Reactivity of M_2-2 with N_2

In order to identify the role of the cation in N_2 binding and reduction we investigated the reaction of **Rb_2-2** and **Cs_2-2** with N_2 and compared it with that previously reported for **K_2-2** (Scheme 2 and S44†).

We previously showed that **K_2-2** reacts rapidly with N_2 in ambient conditions effecting its four-electron reduction and yielding the diuranium(V)–N_2 complex $[K_2\{U^V(OSi(O^tBu)_3)_3\}_2(\mu\text{-}O)(\mu\text{-}N_2)]$, **$K_2$-$N_2$**.

Complex **K_2-N_2** was shown to be stable even under dynamic vacuum although addition of acid or H_2 led to N_2 release. Similarly, when exposing a dark red toluene solution of **Rb_2-2** to 1 atm of N_2, at 25 °C its colour changed suddenly to dark brown and the ^{1}H NMR spectrum showed the disappearance of the signals of the **Rb_2-2** and the appearance a new signal at a chemical shift of −2.27 ppm (Fig. S18†) that was assigned to the N_2 complex $[Rb_2\{U^V(OSi(O^tBu)_3)_3\}_2(\mu\text{-}O)(\mu\text{-}N_2)]$, **$Rb_2$-$N_2$** (Scheme 2).

However, the removal of N_2 from the solution led to the loss of uranium bound dinitrogen and the formation of the **Rb_2-2** complex as shown by ^{1}H NMR studies (Fig. S20†) demonstrating that the binding of **Rb_2-N_2** occurs at ambient pressure and temperature but is reversible under vacuum.

Dark brown crystals of $[Rb_2\{U^V(OSi(O^tBu)_3)_3\}_2(\mu\text{-}O)(\mu\text{-}N_2)]$, **$Rb_2$-$N_2$**, were grown from a concentrated toluene solution under N_2 atmosphere in 53% yield (Scheme 2). However, leaving the isolated solid under dynamic vacuum resulted in dinitrogen loss and in mixtures of **Rb_2-2** and **Rb_2-N_2** complexes (Fig. S19†). Addition of acid or H_2 (Fig. S21†) to **Rb_2-N_2** also resulted only in N_2 loss, as confirmed by the comparison of the ^{1}H NMR spectrum with the reaction of **Rb_2-2** with H_2, which gave the same set of resonances. This was observed previously for the formation of a bis-hydride from **K_2-N_2**.[3h]

In the crystal unit cell of **Rb_2-N_2** (Fig. 2) there are two crystallographically independent molecules. In both molecules an

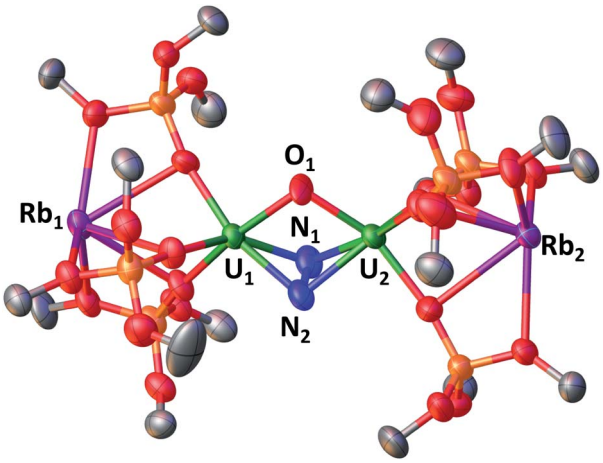

Fig. 2 Solid-state molecular structure of **Rb_2-N_2** (50% probability ellipsoids). Color code: uranium (green), rubidium (purple), oxygen (red), carbon (grey), nitrogen (blue), silicon (orange). Hydrogen atoms and ^{t}Bu groups were omitted for clarity.

oxo group (U1–O–U2 = 104(1)° and U3–O–U4 = 103.7(7)°) and a side-on bound hydrazido moiety (N_2^{4-}) (U1–N2A–U2 = 103.3(2)° and U1–N1A–U2 = 100.5(10)° and U3–N3A–U4 = 102.9(12)° and U1–N1A–U2 = 99.4(5)°) bridge two uranium(V) centers with a short U–U distance of 3.4083(1) Å. As found in the previously reported structure of **K_2-N_2**, the alkali metal cations are not N_2-bound, but are located in the pockets formed by the siloxide moieties.

The $U_2(\mu\text{-}\eta^2\text{-}N_2)$ moiety in **Rb_2-N_2** has U–N distances between 2.14(3) Å and 2.3(1) Å, comparable to those found in **K_2-N_2** and in the previously reported diuranium(V) hydrazido complex $[K_3\{U^V(OSi(O^tBu)_3)_3\}_2(\mu\text{-}N)(\mu\text{-}N_2)]$, K_3UNU.[1j] The N–N bond length in **Rb_2-N_2** (1.41(1) Å) is comparable to that observed in hydrazine, H_2NNH_2 (1.47 Å), and falls in the range of values (1.377–1.548 Å) reported for hydrazido complexes of Zr(IV), U(IV) and U(V).[1h,m,3h,18] The structural parameters point to a formulation of the complex as a $[Rb_2\{U^V(OSi(O^tBu)_3)_3\}_2(\mu\text{-}O)(\mu\text{-}N_2)]$ which is supported by the DFT studies (see infra) and EPR data. Notably, low-temperature (6 K) continuous-wave (CW) X-band EPR of 20 mM toluene solutions of **Rb_2-N_2** measured as toluene/hexane glass (Fig. S82†) revealed the presence of a broad (∼3000 G) and poorly resolved EPR signal, with slightly better distinguished features in the low magnetic field region having the g-factor value of 3.31, which is consistent with a $5f^1$ electronic configuration. Similar g-values have been observed in other uranium(V) complexes.[12m,13e]

The structural and EPR data suggest a similar degree of activation of the bound N_2 occurring in **Rb_2-N_2** and **K_2-N_2**, but release of N_2 occurs for **Rb_2-N_2** under vacuum.

The lower stability of the N_2 complex **Rb_2-N_2** compared to **K_2-N_2** under vacuum indicates a decreased binding constant of the N_2 complex despite the structural similarity of the two U(III) complexes **Rb_2-2** and **K_2-2** and their N_2 complexes **K_2-N_2** and **Rb_2-N_2** (see structural description above). It should also be noted that although the alkali ion does not bind directly the N_2

in the solid-state structure of the final N_2 complex, it plays an important role in N_2 binding.

Finally, ^{1}H NMR studies show that when exposing solid **Cs_2-2** or a toluene solution to 1 atm of N_2 at 25 °C or lower temperatures (−40 °C or −80 °C) no reaction is observed. The addition of higher pressures of N_2 (10 to 100 bar) at 25 °C to a dark red toluene solution of **Cs_2-2** did not yield any new species, as confirmed by ^{1}H NMR studies (Fig. S41†). However, exposing a dark red solution of **Cs_2-2** to higher pressures (12–100 atm) of N_2 at −40 °C resulted in the partial to total consumption of the U(III) starting material and the formation of a new species as confirmed by ^{1}H NMR studies showing one broad signal for the siloxide ligands similarly to what found for the **K_2-N_2** and **Rb_2-N_2** complexes, (Fig. S42–S44†). The binding of dinitrogen is reversible when removing the excess pressure at −40 °C, forming **Cs_2-2** over the course of 16 h (Fig. S43†). When increasing the temperature at 100 atm formation of **Cs_2-2** is also observed together with unidentified decomposition products. Favourable binding of N_2 at low temperature has been previously observed for titanium and lanthanide complexes.[19]

These results show the important effect of the coordinated cation in the binding of dinitrogen by the dinuclear oxo bridged diuranium(III) complexes $[M_2\{[U^{III}(OSi(O^tBu)_3)_3\}_2(\mu\text{-}O)]$, **$M_2$-2**. In particular, an important decrease in N_2 binding affinity is observed from K^+ to Rb^+ to Cs^+ that can be correlated with the increased size and decreased Lewis acidity of the cation. The electronic effects of the bound cation on the reactivity of the diuranium(III) complex are not straightforward since an increased Lewis acidity of the cation should result in a less electron-donating siloxide ligand and as a result a less reducing uranium center which was confirmed by cyclic voltammetry studies (see infra).

Steric effects arising from the presence of a larger cation binding the siloxide could also play a role. Notably, the larger size of the Cs^+ compared to K^+ and the binding of two Cs^+ to the bridging oxide results in an overall arrangement that renders more difficult or even prevents the access to the U centers, as can be seen for the space filling diagrams of the **M_2-2** complexes (Fig. S56†) and by computational data (Fig. 5).

Although the alkali ions do not bind dinitrogen in the final **M_2-N_2** complexes, cation binding to the reduced U(III)–O–U(III) complex affects significantly the ability of the metal centers to bind and reduce N_2. Since differences in N_2 binding arise from the different binding of alkali cations to the oxo linkers, we believe these results bear some relevance to the Haber–Bosch process since the Mittasch catalyst is based on metal oxides.

Indeed, besides the steric effects of the molecular siloxide envelope, this study hints that the binding of larger ions such as Cs to the M–O–M fragment is likely to reduce the N_2 binding constant in metal oxides.

Electrochemical studies

To fully characterize and compare the reduction power of the **M_2-2** complexes, cyclic voltammetry data were measured under argon atmosphere for these complexes and for complex **1** in ~0.1 M THF solution of $[Bu_4N][BPh_4]$ and are presented in Fig. 3. All redox potentials are referenced against the $[(C_5H_5)_2Fe]^{+/0}$ redox couple.

The voltammogram of complex **1** shows a distinctive irreversible reduction event at $E_{pc} = -3.32$ V associated with the irreversible oxidation process at $E_{pa} = -2.48$ V. This irreversible redox event can be associated to the U(III)/U(IV) couple, since the oxidation at $E_{pa} = -2.48$ V is not observed in the voltammogram of **1** when it is swept initially from −1.98 V towards the positive region.

The same irreversible redox events were observed in the voltammograms of the family of complexes **M_2-2**. Interestingly, a distinctive oxidation event ($E_{pc} = -2.3$, −2.37 and −2.41 V for M = K, Rb and Cs, respectively) is observed always when swept towards positive region, which shifts towards negative values when decreasing the Lewis acidity of M. The respective reduction event ($E_{pc} = -3.07$, −3.23 and −3.4 V for M = K, Rb and Cs, respectively) is only observed after initial oxidation of the complexes and a negative shift is also observed when decreasing the Lewis acidity of M (Table 2).

These results show that the reducing potential of **M_2-2** increases with the decrease in the Lewis acidity of the alkali metal counterion, with the highest reducing power for the series observed for **Cs_2-2** ($E_{pc} = -3.4$ V and $E_{pa} = -2.41$ V).

The values of the redox potentials assigned to the redox couple U(IV)/U(III) in **M_2-2** are significantly more negative than

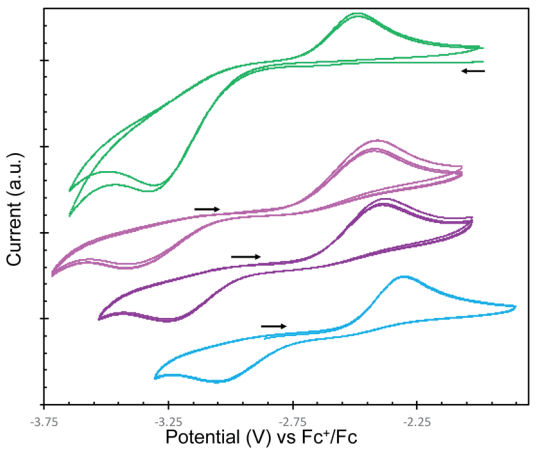

Fig. 3 [−3.8 V; −1.85 V] region of cyclic voltammogram of THF solutions of complexes **1** (3.0 mM, green) and **M_2-2** (3.5 mM, M = Cs, pink), (3.0 mM, M = Rb, purple), (3.0 mM, M = K, light blue) recorded in 0.1 M $[NBu_4][BPh_4]$ under Ar at 25 °C, at a scan rate of 100 mV s^{-1}, referenced against $[Fe(C_5H_5)_2]^{+/0}$.

Table 2 Reduction potentials assigned to the U(IV)/U(III) couples in this study

Compound	E_{pc} (V)	E_{pa} (V)	ΔE (V)
1	−3.32	−2.48	0.84
Cs_2-2	−3.4	−2.41	0.99
Rb_2-2	−3.23	−2.37	0.86
K_2-2	−3.07	−2.3	0.77

previously reported values for the same redox couple in a family of cyclopentadienyl U(III) complexes (in the range between −1.04 V and −1.54 V).[20] These results show that siloxide supported diuranium(III) oxides are highly reducing, but also indicate that the difference in reactivity towards dinitrogen observed for the **M_2-2** complexes cannot be related to differences in redox potential of the uranium centers. Notably the most reducing complex **Cs_2-2** is showing the lowest reactivity with N_2.

Dinitrogen cleavage and functionalization by Rb_2-2 and Cs_2-2

We recently reported that the reduction of the N_2 complex **K_2-N_2** with 2 equiv. of KC_8 leads to the formation of a new species with a higher degree of activation of the bound N_2. On the basis of the structure of the tetranitride complex isolated from the reduction of **K_2-N_2** with excess KC_8 and on the basis of computational and reactivity studies this species was proposed to be a bis-nitride complex but its molecular structure was not elucidated.[4c]

To gain further insight into the role of the alkali ions in the cleavage of N_2 to nitrides we explored the reduction of **Rb_2-N_2** with 2 equiv. RbC_8 and of **Rb_2-2** and **Cs_2-2** with 2 equiv. RbC_8 and CsC_8 respectively under N_2.

^{1}H NMR studies (Fig. S34 and S35†) showed that the reduction of **Rb_2-N_2** with 2 equiv. of RbC_8 at −40 °C under 1 atmosphere N_2 or the reduction of **Rb_2-2** with 2 equiv. RbC_8 under 1 atmosphere N_2 lead to the formation of a new species which displays ^{1}H NMR signals similar to those reported for the putative bis-nitride intermediate obtained from the 2 electron reduction of **K_2-N_2** (Fig. S36–S39†).[4c] Unfortunately also in this case the putative nitride could not be isolated from the reaction mixture. However, the addition of excess acid to the reaction mixture between **Rb_2-2** and 2 equiv. of RbC_8 after removing the graphite yielded NH_4Cl in 85% yield (1.7 equiv., 100% conversion corresponding to 2 equiv. of NH_4Cl) suggesting that cleavage of the bound N_2 has occurred.

Despite the fact that we were not able to observe N_2 binding by **Cs_2-2** at −40 °C and 1 atm N_2 by ^{1}H NMR spectroscopy we could not completely rule out the possibility of weak N_2 binding not observable by NMR.[19c,21]

Gratifyingly the reduction of **Cs_2-2** with 2 equiv. of CsC_8 at −40 °C under 1 atmosphere of N_2 revealed the complete consumption of the dinuclear U(III) starting material and the formation of a new major species (Fig. S22 and S23†). Golden-yellow crystals of $[Cs_3\{U^V(OSi(O^tBu)_3)_3\}(\mu\text{-}N)_2\{U^V(OSi(O^tBu)_3)_2(\kappa\text{-}O)\}][CsOSi(O^tBu)_3]$ **Cs_4-$(N)_2$** (Fig. 4) were grown in 50% yield by leaving a concentrated toluene solution of **Cs_4-$(N)_2$** at −40 °C over the course of two days (Scheme 3). ^{1}H NMR studies indicated that the same reaction performed under an Ar atmosphere, did not lead to new reduction products but only to formation of small traces of decomposition (Fig. S28†).

These results suggest that reversible binding of N_2 by **Cs_2-2** must occur to some extent in toluene solution also at −40 °C and 1 atm although it was not possible to detect it by ^{1}H NMR spectroscopy.

Cs_4-$(N)_2$ is unstable in toluene solution at 25 °C, decomposing completely over the course of 12 h (Fig. S26†). The decomposition is slower at −40 °C, with 75% of **Cs_4-$(N)_2$** still present in solution after 2 weeks (Fig. S27†).

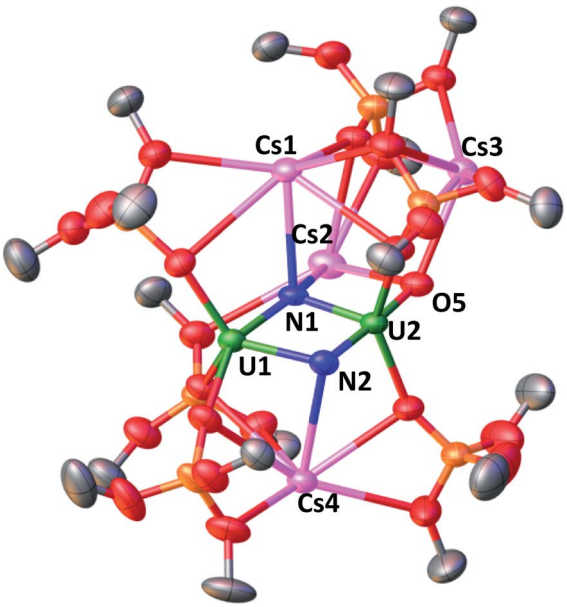

Fig. 4 Solid-state molecular structure of **Cs_4-$(N)_2$** (50% probability ellipsoids). Color code: uranium (green), cesium (pink), oxygen (red), carbon (grey), nitrogen (blue), silicon (orange). Hydrogen atoms and ^{t}Bu groups were omitted for clarity.

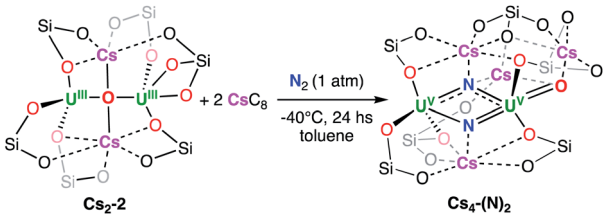

Scheme 3 Reduction of **Cs_2-2** under N_2.

The molecular structure of complex **Cs_4-$(N)_2$** (Fig. 4) shows the presence of two independent dimeric complexes where two uranium ions and three cesium ions are bridged by two nitrides (the μ_4-nitride N1 bridges two U centers and two Cs and the μ_3-nitride N2 bridges two U and one Cs). The two U(v) centers are both pentacoordinated with a distorted square pyramidal geometry and are held together by the bridging nitrides and the siloxide framework at a short U–U distance of 3.337(2) Å. U1 is coordinated by two oxygen atoms from the siloxide ligands, the two nitrides and a terminal oxo group, while U2 is coordinated by three oxygen atoms from the siloxide ligands and two nitrides.

Asymmetric U–N bond distances are found in complex **Cs_4-$(N)_2$**. In particular, a very short U–N distance (U2–N2 = 1.85(1) Å) and a longer U–N distance (U1–N2 = 2.34(1) Å) is found for the (μ_3-nitride) which is *trans* to the terminal oxo group, which suggest that N2 binds U2 with a multiple bond and U1 with a single bond. The (μ_4-nitride) bridges the two U(v) centers in

a more symmetric fashion (U–N1: 2.09(1) Å and 2.13(1) Å). The latter distances compare well to those found in the previously reported dinuclear U(IV)/U(V) (U–N: 2.076(6) and 2.099(5) Å),[4a] and the U(V)/U(V) bis-nitrides (U–N: 2.101(6) and 2.022(5) Å) complexes.[13a]

The terminal oxo O5 binds two cesium atoms resulting in a U1–O5 distance (1.856(4) Å) longer than the one observed in the previously reported U(V) terminal oxo [U(O){N(Si(Me$_3$))$_2$}$_3$] (U–O distance 1.817(1) Å).[22] The complex **Cs$_4$-(N)$_2$** presents a unique and second of its kind nitride-substituted analogue of the uranyl(V) ion. The distances observed in the *trans* oxo-nitrido moiety [O=U^V=N] found in **Cs$_4$-(N)$_2$** (U2–O5: 1.856(4) Å; U2–N2 = 1.85(1) Å) are significantly longer than those found in the only other known *trans* oxo-nitrido U(VI) complex reported by Hayton and coworkers[12c] (U–O = 1.797(7) Å; U–N = 1.818(9) Å).

An additional siloxide ligand is held in the complex through the binding of three Cs cations. The shift of the bridging oxo to terminal oxo is likely to be responsible for the cleavage of the U2–OSi(O^{t}Bu)$_3$ bond.

^{1}H NMR studies show that most of the Cs-bound siloxide ligand remains associated in toluene solution but dissociation was observed in THF (Fig. S31–S33†).

Variable temperature SQUID magnetic data were measured in the temperature range 2 K–250 K for **Cs$_4$-(N)$_2$** (due to the low stability of the complex at room temperature) and compared with the previously reported putative "**K$_4$-(N)$_2$**" intermediate. The measured magnetic data of **Cs$_4$-(N)$_2$** are similar to those measured *in situ* for the putative "**K$_4$-(N)$_2$**"[4c] with a magnetic moment per ion of μ = 1.51 μ_B at 250 K for "**K$_4$-(N)$_2$**" and of μ = 1.57 μ_B at 250 K for **Cs$_4$-(N)$_2$** and μ = 0.33 μ_B for **Cs$_4$-(N)$_2$** and μ = 0.27 μ_B for "**K$_4$-(N)$_2$**" at 2 K, indicative of the presence of U(V) cations, and a χ *versus* T behaviour in agreement with the presence of two magnetically independent ions (Fig. S66†), similarly to what was found for "**K$_4$-(N)$_2$**".

^{1}H NMR studies showed that the *in situ* reduction of the diuranium(IV) complex **1** with 4 equiv. of CsC_8 in toluene at −40 °C carried out under N_2 resulted in the formation of the bis-nitride complex **Cs$_4$-(N)$_2$** as the major species after 24 hours (Fig. S53†) *via* the **Cs$_2$-2** intermediate (Fig. S54†). Previous studies had shown that reduction of **1** with 4 equiv. of KC_8 in toluene at −40 °C resulted in the formation of multiple products due to different redox reactions occurring at the same time.[4c]

The reactivity of the nitrides in **Cs$_4$-(N)$_2$** with electrophiles (H^+ and CO) was then probed.

The addition of excess HCl(Et$_2$O) to isolated **Cs$_4$-(N)$_2$** yielded NH_4Cl in 100% yield (Fig. S30†). The addition of excess acid to the reaction mixture between **Cs$_2$-2** and 2 equiv. of CsC_8 under N_2 after removing the graphite yielded NH_4Cl in 83% yield (1.66 equiv., 100% conversion corresponding to 2 equiv. of NH_4Cl).

These results show that the bis-nitride formed from N_2 reaction reacts readily with protons to give ammonia.

The addition of excess ^{13}CO (5 equiv.) to **Cs$_4$-(N)$_2$** resulted in the formation of the diuranium(IV) bis-oxo complex [Cs$_2${[-U^{IV}(OSi(O^{t}Bu)$_3$)$_3$]$_2$(μ-O)$_2$}], **Cs$_2$-4** (Scheme 4) in 91% yield as shown by ^{1}H NMR studies (Fig. S48†) and single crystal X-ray diffraction (Fig. S60†). Moreover, the ^{13}C NMR spectrum of

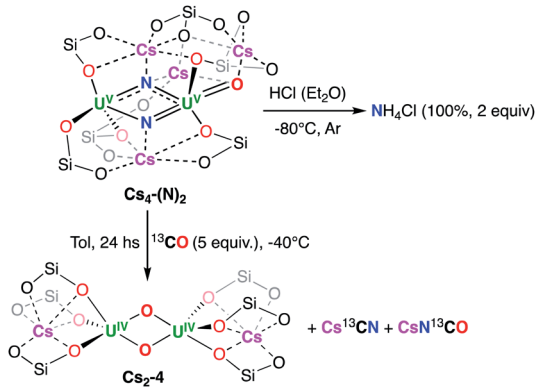

Scheme 4 Reactivity of Cs$_4$-(N)$_2$.

the reaction mixture quenched in D_2O shows the presence of Cs^{13}CN and CsN^{13}CO in 1 : 1 ratio with overall yield of 100%.

The formation of the bis-oxo and Cs^{13}CN indicates that one bridging nitride promotes the cleavage and deoxygenation of carbon monoxide to afford a N–C triple bond and a bridging oxo group. A second molecule of CO effects the reductive carbonylation of the second nitride to yield a diuranium(IV) bis-oxo complex, **Cs$_2$-4** and isocyanate. Rare examples of nitride functionalization by CO[23] including CO cleavage by uranium nitrides have been reported previously.[24] Notably similar reactivity with CO was observed for the putative diuranium(V) nitride analogue "**K$_4$-(N)$_2$**"[4c] and for the previously reported diuranium(V) bis-nitride prepared by reaction of U(III) with alkali azides.[13a]

Computational studies

To get some insights on the effect of the different alkali atoms, DFT calculations (B3PW91) were carried out. Complexes **K$_2$-2**, **Rb$_2$-2** and **Cs$_2$-2** were first optimized. Interestingly, for **Cs$_2$-2**, it has been possible to obtain both a ferromagnetic and antiferromagnetic (AF) coupling, that were found to be at the same energy (0.2 kcal mol^{-1} difference with AF slightly lower in energy), whereas only a ferromagnetic coupling was obtained for the other complexes. The bonding was analysed in these three complexes and a U=O double bond is found (see ESI† for details). The U=O double bonds are found in the three complexes to be strongly polarized toward O (93% in **K$_2$-2**, 90% in **Rb$_2$-2** and 83% in **Cs$_2$-2**). Thus, the U=O bonds are slightly more covalent in the latter complex in line with the linear structure of the oxo. Then, the binding of N_2 was investigated in the three cases and three stable structures **K$_2$-N$_2$**, **Rb$_2$-N$_2$** and **Cs$_2$-N$_2$** were obtained. The binding energy of N_2 was thus computed and is found to decrease (−19.4 kcal mol^{-1} for K, −5.1 kcal mol^{-1} for Rb and finally −0.1 kcal mol^{-1} for Cs) for increasing values of the cation atomic number Z and decreased charge density on the alkali ion. These values are in line with the experiments since the binding is irreversible for K, reversible for Rb in ambient conditions and binding occurs for Cs only at high pressure and low temperature.

This difference of N_2 binding is attributed to steric effects since no clear electronic differences in the three systems **K$_2$-2**,

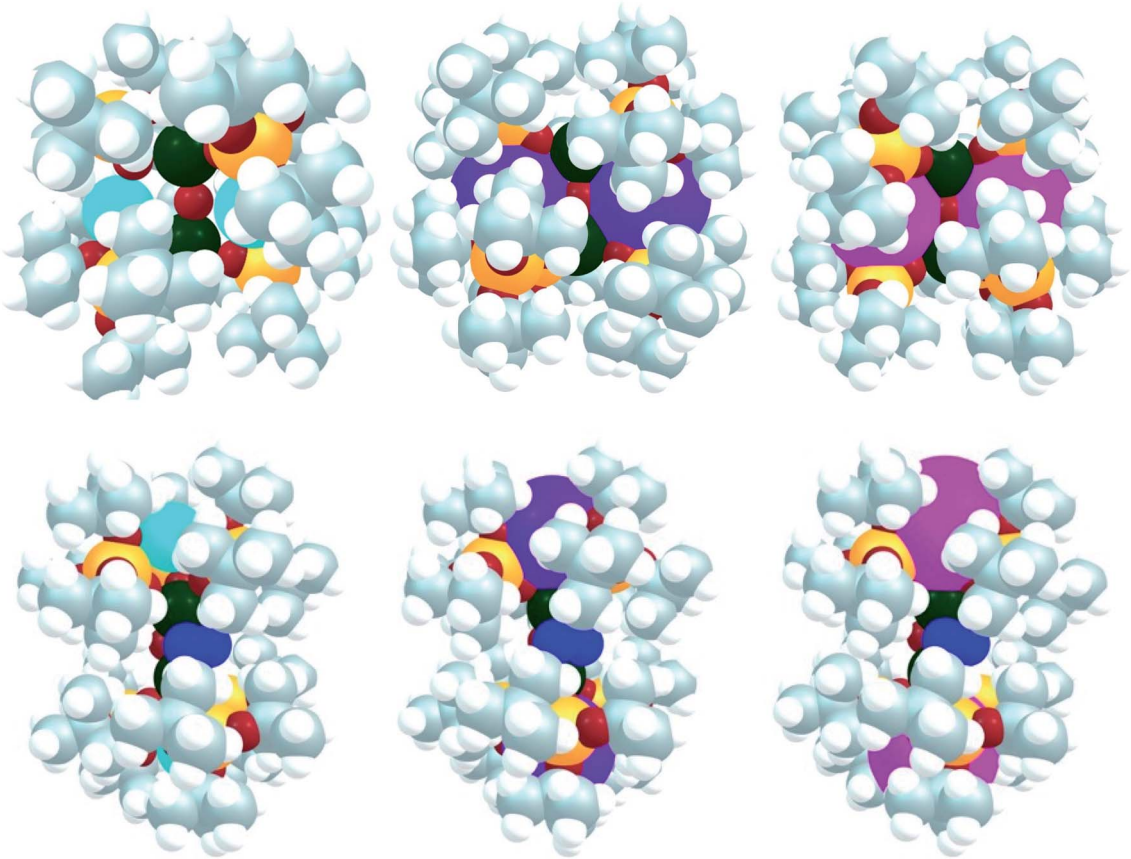

Fig. 5 Big atom representation of K_2-2, Rb_2-2 and Cs_2-2 (top) as well as K_2-N_2, Rb_2-N_2 and Cs_2-N_2 (bottom).

Rb_2-2 and **Cs_2-2** are found (*e.g.* the U charge is 1.62 and the K one is 0.96 **K_2-2**, 1.65 for U and 0.96 for Rb in **Rb_2-2** and 1.59 for U and 1.02 for Cs in **Cs_2-2**, see ESI† for a complete report of the density analysis).

It is interesting to note that the charge at U is the lowest in **Cs_2-2** where the charge of the alkali atom is the largest, indicating that U is more basic. This is in line with the electrochemistry where U is slightly more reducing in **Cs_2-2** than in **K_2-2.** Indeed, the N_2 binding in **Cs_2-N_2** would clearly induce a steric clash in the complex while it is pronounced in the two other cases. This is highlighted in Fig. 5 where a "big atom" representation of the optimized structures of **K_2-2**, **Rb_2-2** and **Cs_2-2** (top) as well as **K_2-N_2**, **Rb_2-N_2** and **Cs_2-N_2** (bottom) is provided (in this representation each atom is drawn according to its atomic radius). In all cases, the bound dinitrogen molecule is found to be N_2^{4-} in line with the presence of two U(v) (see unpaired electron density in ESI†).

Finally, the full reduction of N_2, that is the formation of complexes **M_4-$(N)_2$** with M = K, Rb, Cs, was investigated computationally. A stable structure was optimized in the three cases and the enthalpy of formation of **M_4-$(N)_2$** from **M_2-2** is ranging from −83.1 kcal mol^{-1} (M = Rb) to −91.9 kcal mol^{-1} (M = K). This is in line with the experiment and the slow conversion (24 hours) for **Cs_2-2** is due to the very low binding affinity of N_2 (Fig. 6).

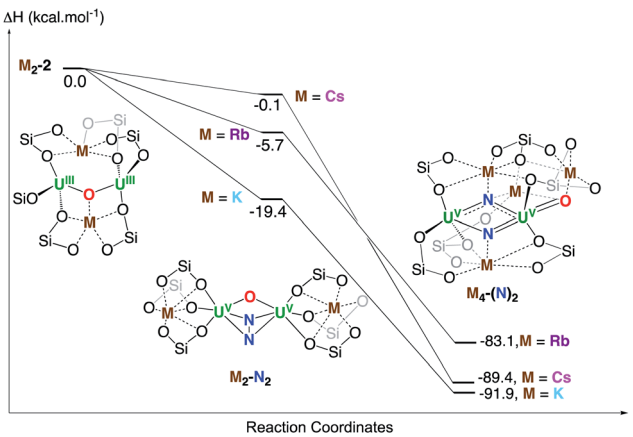

Fig. 6 Computed enthalpy profile in kcal mol^{-1} at room temperature for the formation of K_4-$(N)_2$, Rb_4-$(N)_2$ and Cs_4-$(N)_2$ from the reduction of N_2 by K_2-N_2, Rb_2-N_2 and Cs_2-N_2 respectively.

The bonding in **Cs_4-$(N)_2$** (Fig. S7†) was analysed using the Natural Bonding Analysis (NBO). The presence of an almost linear N–U–O moiety (172°) is of particular interest in **Cs_4-$(N)_2$**. The bonding in this fragment is very similar to what found for uranyl ion with a set a U–O triple bond and a set of U–N triple bond. The three U–O bonds ($1\sigma + 2\pi$) are strongly polarized toward O(81%) and involve an overlap between df orbitals on U

(47% 6d + 53% 5f)and sp on O. A relatively similar bonding mode is observed for the U–N triple bond. However, the bond is slightly less polarized toward N (71% *vs.* 81% for O). These bonds also imply overlap between df hybrid orbital on U (roughly 50–50) and sp orbital on N. The fact that these bonds are strongly polarized explains the relatively low WBI found (0.31 for UN and 0.14 for UO). The second nitride is found to mainly bind to the second uranium with also a triple bond.

Conclusions

Here we compared the structural, redox and magnetic properties of a unique series of structurally analogous multimetallic complexes of low valent uranium where an oxide bridge connects two U(III) centers and two alkali ions of different nature $[M_2\{U^{III}(OSi(O^tBu)_3)_3\}_2(\mu\text{-}O)]$ (M = K, **K_2-2**; Rb, **Rb_2-2**; M = Cs, **Cs_2-2**). Overall, the binding of the cations K, Rb and Cs in the three complexes is quite similar, with the main differences being the coordination of two Cs^+ to the bridging oxide compared to only one K^+ or Rb^+ and the resulting symmetric and linear U–O–U arrangement in **Cs_2-2** compared to an asymmetric and bent U–O–U in the K and Rb analogues. These differences result in different magnetic properties with a weak antiferromagnetic coupling observed between the U(III) ions in **Cs_2-2** while the two U(III) behave as independent paramagnets in **K_2-2** and **Rb_2-2**. Cyclic voltammetry measurements show an increasing reducing power for the U(III) ions with the increasing ionic radii of the alkali ion and subsequent reduced charge density (K < Rb < Cs). The three complexes show a very different binding ability towards dinitrogen which decreases with the increasing size of the alkali ion and is therefore not correlated to the difference in redox potential. Notably the **K_2-2** complex binds irreversibly N_2 in ambient conditions (1 atm and 25 °C) while N_2 binding is reversible for **Rb_2-2** in the same conditions and only occurs at high pressures (100 atm) and low temperatures (−40 °C) for **Cs_2-2**. DFT analysis indicated that N_2 binding by **Cs_2-2** is hindered by steric effects, but the structures computed for the **M_2-N_2** species show a similar degree of activation of bound N_2 for all cations. Remarkably, although N_2 binding could not be detected in ambient conditions, reduction of **Cs_2-2** under N_2 led to the first example of cesium assisted N_2 cleavage by a metallic complex. The molecular structure of the N_2 cleavage product **Cs_4-$(N)_2$** presents two Cs-bound nitrides binding two U(V) in a diamond-shaped arrangement while the bridging oxide has switched to a terminal binding mode. Furthermore, the two nitrides are readily and quantitatively functionalized by protons and CO. This study provided a relevant molecular model for N_2 binding in metal oxides and suggests that structural effects dominate the effect of alkali ions in N_2 binding. We also showed that strong binding is not required for further reduction of N_2 to nitride which can also be effected by cesium cations.

Data availability

All data were given in ESI and CCDC.†

Author contributions

N. J. carried out all the synthetic experiments and analyzed the experimental data. R. S. carried out the X-ray single crystal structure analyses. I. Z. collected the variable-temperature magnetic data. A. S. recorded and analyzed the EPR data. T. R. and L.M. carried out the computational studies. M. M. originated the central idea, coordinated the work, and analyzed the experimental data. The manuscript was written through contributions of all authors.

Conflicts of interest

There are no conflicts to declare.

Acknowledgements

We acknowledge support from the Swiss National Science Foundation grant number 178793 and the Ecole Polytechnique Fédérale de Lausanne (EPFL). We thank Farzaneh Fadaei-Tirani for important contributions to the X-ray single crystal structure analyses. We thank Dr David Savary in the group of Prof. Paul Dyson for its help with the high-pressure experiments. We thank Roxane Moinat for carrying out the elemental analyses. L. M. is a senior member of the Institut Universitaire de France. CalMip is acknowledged for a generous grant of computing time.

References

1 (*a*) I. Castro-Rodriguez, H. Nakai, L. N. Zakharov, A. L. Rheingold and K. Meyer, *Science*, 2004, **305**, 1757–1759; (*b*) S. C. Bart and K. Meyer, in *Structure and Bonding*, 2008, vol. 127, pp. 119–176; (*c*) M. S. Eisen, *Top. Organomet. Chem.*, 2010, **31**, 157–184; (*d*) O. Cooper, C. Camp, J. Pecaut, C. E. Kefalidis, L. Maron, S. Gambarelli and M. Mazzanti, *J. Am. Chem. Soc.*, 2014, **136**, 6716–6723; (*e*) I. S. R. Karmel, N. Fridman, M. Tamm and M. S. Eisen, *J. Am. Chem. Soc.*, 2014, **136**, 17180–17192; (*f*) H. S. La Pierre and K. Meyer, in *Progress in Inorganic Chemistry*, ed. K. D. Karlin, 2014, vol. 58, pp. 303–415; (*g*) D. P. Halter, F. W. Heinemann, J. Bachmann and K. Meyer, *Nature*, 2016, **530**, 317–321; (*h*) M. D. Walter, *Adv. Organomet. Chem.*, 2016, **65**, 261–377; (*i*) P. L. Arnold and Z. R. Turner, *Nat. Rev. Chem.*, 2017, **1**, 0002; (*j*) M. Falcone, L. Chatelain, R. Scopelliti, I. Zivkovic and M. Mazzanti, *Nature*, 2017, **547**, 332–335; (*k*) H. Liu, T. Ghatak and M. S. Eisen, *Chem. Commun.*, 2017, **53**, 11278–11297; (*l*) L. Barluzzi, M. Falcone and M. Mazzanti, *Chem. Commun.*, 2019, **55**, 13031–13047; (*m*) P. L. Arnold, T. Ochiai, F. Y. T. Lam, R. P. Kelly, M. L. Seymour and L. Maron, *Nat. Chem.*, 2020, **12**, 654–659; (*n*) M. A. Boreen and J. Arnold, *J. Chem. Soc., Dalton Trans.*, 2020, **49**, 15124–15138; (*o*) D. R. Hartline and K. Meyer, *JACS Au*, 2021, **1**, 698–709.

2 (*a*) F. Haber, Ammonia, *German Pat.*, DE229126, 1909; (*b*) F. Haber, *Angew. Chem.*, 1914, **27**, 473–477.

3 (*a*) A. L. Odom, P. L. Arnold and C. C. Cummins, *J. Am. Chem. Soc.*, 1998, **120**, 5836–5837; (*b*) P. Roussel and P. Scott, *J. Am. Chem. Soc.*, 1998, **120**, 1070–1071; (*c*) G. F. N. Cloke and P. B. Hitchcock, *J. Am. Chem. Soc.*, 2002, **124**, 9352–9353; (*d*) W. J. Evans, S. A. Kozimor and J. W. Ziller, *J. Am. Chem. Soc.*, 2003, **125**, 14264–14265; (*e*) S. M. Mansell, N. Kaltsoyannis and P. L. Arnold, *J. Am. Chem. Soc.*, 2011, **133**, 9036–9051; (*f*) S. M. Mansell, J. H. Farnaby, A. I. Germeroth and P. L. Arnold, *Organometallics*, 2013, **32**, 4214–4222; (*g*) M. D. Walter, *Adv. Organomet. Chem.*, 2016, **65**, 261–377; (*h*) M. Falcone, L. Barluzzi, J. Andrez, F. F. Tirani, I. Zivkovic, A. Fabrizio, C. Corminboeuf, K. Severin and M. Mazzanti, *Nat. Chem.*, 2019, **11**, 154–160; (*i*) E. Lu, B. E. Atkinson, A. J. Wooles, J. T. Boronski, L. R. Doyle, F. Tuna, J. D. Cryer, P. J. Cobb, I. J. Vitorica-Yrezabal, G. F. S. Whitehead, N. Kaltsoyannis and S. T. Liddle, *Nat. Chem.*, 2019, **11**, 806–811; (*j*) D. Singh, W. R. Buratto, J. F. Torres and L. J. Murray, *Chem. Rev.*, 2020, **120**, 5517–5581.

4 (*a*) I. Korobkov, S. Gambarotta and G. P. A. Yap, *Angew. Chem., Int. Ed. Engl.*, 2002, **41**, 3433–3436; (*b*) X. Q. Xin, I. Douair, Y. Zhao, S. Wang, L. Maron and C. Q. Zhu, *J. Am. Chem. Soc.*, 2020, **142**, 15004–15011; (*c*) N. Jori, L. Barluzzi, I. Douair, L. Maron, F. Fadaei-Tirani, I. Zivkovic and M. Mazzanti, *J. Am. Chem. Soc.*, 2021, **143**, 11225–11234.

5 (*a*) C. E. Laplaza and C. C. Cummins, *Science*, 1995, **268**, 861–863; (*b*) S. Gambarotta and J. Scott, *Angew. Chem., Int. Ed. Engl.*, 2004, **43**, 5298–5308; (*c*) M. M. Rodriguez, E. Bill, W. W. Brennessel and P. L. Holland, *Science*, 2011, **334**, 780–783; (*d*) T. Shima, S. W. Hu, G. Luo, X. H. Kang, Y. Luo and Z. M. Hou, *Science*, 2013, **340**, 1549–1552; (*e*) K. P. Chiang, S. M. Bellows, W. W. Brennessel and P. L. Holland, *Chem. Sci.*, 2014, **5**, 267–274; (*f*) K. Grubel, W. W. Brennessel, B. Q. Mercado and P. L. Holland, *J. Am. Chem. Soc.*, 2014, **136**, 16807–16816; (*g*) G. P. Connor and P. L. Holland, *Catal. Today*, 2017, **286**, 21–40; (*h*) L. R. Doyle, A. J. Wooles and S. T. Liddle, *Angew. Chem., Int. Ed. Engl.*, 2019, **58**, 6674–6677; (*i*) M. J. Dorantes, J. T. Moore, E. Bill, B. Mienert and C. C. Lu, *Chem. Commun.*, 2020, **56**, 11030–11033; (*j*) S. J. K. Forrest, B. Schluschass, E. Y. Yuzik-Klimova and S. Schneider, *Chem. Rev.*, 2021, **121**, 6522–6587; (*k*) F. Masero, M. A. Perrin, S. Dey and V. Mougel, *Chem.–Eur. J.*, 2021, **27**, 3892–3928.

6 (*a*) R. Krabetz and C. Peters, *Angew. Chem., Int. Ed. Engl.*, 1965, **4**, 341–347; (*b*) H. P. Jia and E. A. Quadrelli, *Chem. Soc. Rev.*, 2014, **43**, 547–564.

7 (*a*) P. L. Holland, *J. Chem. Soc., Dalton Trans.*, 2010, **39**, 5415–5425; (*b*) J. B. Geri, J. P. Shanahan and N. K. Szymczak, *J. Am. Chem. Soc.*, 2017, **139**, 5952–5956.

8 W. J. Evans, M. Fang, G. Zucchi, F. Furche, J. W. Ziller, R. M. Hoekstra and J. I. Zink, *J. Am. Chem. Soc.*, 2009, **131**, 11195–11202.

9 M. Fang, D. S. Lee, J. W. Ziller, R. J. Doedens, J. E. Bates, F. Furche and W. J. Evans, *J. Am. Chem. Soc.*, 2011, **133**, 3784–3787.

10 (*a*) R. Ferguson, E. Solari, C. Floriani, D. Osella, M. Ravera, N. Re, N. ChiesiVilla and C. Rizzoli, *J. Am. Chem. Soc.*, 1997, **119**, 10104–10115; (*b*) G. K. B. Clentsmith, V. M. E. Bates, P. B. Hitchcock and F. G. N. Cloke, *J. Am. Chem. Soc.*, 1999, **121**, 10444–10445; (*c*) A. Caselli, E. Solari, R. Scopelliti, C. Floriani, N. Re, C. Rizzoli and A. Chiesi-Villa, *J. Am. Chem. Soc.*, 2000, **122**, 3652–3670; (*d*) H. Kawaguchi and T. Matsuo, *Angew. Chem., Int. Ed. Engl.*, 2002, **41**, 2792–2794; (*e*) G. Ung and J. C. Peters, *Angew. Chem., Int. Ed. Engl.*, 2015, **54**, 532–535; (*f*) T. D. Lohrey, R. G. Bergman and J. Arnold, *J. Chem. Soc., Dalton Trans.*, 2019, **48**, 17936–17944; (*g*) S. Suzuki, Y. Ishida, H. Kameo, S. Sakaki and H. Kawaguchi, *Angew. Chem., Int. Ed. Engl.*, 2020, **59**, 13444–13450.

11 (*a*) S. F. McWilliams and P. L. Holland, *Acc. Chem. Res.*, 2015, **48**, 2059–2065; (*b*) K. C. MacLeod, F. S. Menges, S. F. McWilliams, S. M. Craig, B. Mercado, M. A. Johnson and P. L. Holland, *J. Am. Chem. Soc.*, 2016, **138**, 11185–11191.

12 (*a*) W. J. Evans, S. A. Kozimor and J. W. Ziller, *Science*, 2005, **309**, 1835–1838; (*b*) G. Nocton, J. Pecaut and M. Mazzanti, *Angew. Chem., Int. Ed. Engl.*, 2008, **47**, 3040–3042; (*c*) S. Fortier, G. Wu and T. W. Hayton, *J. Am. Chem. Soc.*, 2010, **132**, 6888–6889; (*d*) A. R. Fox, P. L. Arnold and C. C. Cummins, *J. Am. Chem. Soc.*, 2010, **132**, 3250–3251; (*e*) R. K. Thomson, T. Cantat, B. L. Scott, D. E. Morris, E. R. Batista and J. L. Kiplinger, *Nat. Chem.*, 2010, **2**, 723–729; (*f*) T. K. Todorova, L. Gagliardi, J. R. Walensky, K. A. Miller and W. J. Evans, *J. Am. Chem. Soc.*, 2010, **132**, 12397–12403; (*g*) D. M. King, F. Tuna, E. J. L. McInnes, J. McMaster, W. Lewis, A. J. Blake and S. T. Liddle, *Science*, 2012, **337**, 717–720; (*h*) C. Camp, J. Pecaut and M. Mazzanti, *J. Am. Chem. Soc.*, 2013, **135**, 12101–12111; (*i*) D. M. King, F. Tuna, E. J. L. McInnes, J. McMaster, W. Lewis, A. J. Blake and S. T. Liddle, *Nat. Chem.*, 2013, **5**, 482–488; (*j*) D. M. King and S. T. Liddle, *Coord. Chem. Rev.*, 2014, **266**, 2–15; (*k*) L. Maria, I. C. Santos, V. R. Sousa and J. Marcalo, *Inorg. Chem.*, 2015, **54**, 9115–9126; (*l*) L. Chatelain, R. Scopelliti and M. Mazzanti, *J. Am. Chem. Soc.*, 2016, **138**, 1784–1787; (*m*) D. M. King, P. A. Cleaves, A. J. Wooles, B. M. Gardner, N. F. Chilton, F. Tuna, W. Lewis, E. J. L. McInnes and S. T. Liddle, *Nat. Commun.*, 2016, **7**, 13773; (*n*) N. Tsoureas, A. F. R. Kilpatrick, C. J. Inman and F. G. N. Cloke, *Chem. Sci.*, 2016, **7**, 4624–4632; (*o*) K. C. Mullane, H. Ryu, T. Cheisson, L. N. Grant, J. Y. Park, B. C. Manor, P. J. Carroll, M. H. Baik, D. J. Mindiola and E. J. Schelter, *J. Am. Chem. Soc.*, 2018, **140**, 11335–11340; (*p*) L. Barluzzi, N. Jori, T. Y. He, T. Rajeshkumar, R. Scopelliti, L. Maron, P. Oyala, T. Agapie and M. Mazzanti, *Chem. Commun.*, 2022, **58**, 4655–4658.

13 (*a*) L. Barluzzi, L. Chatelain, F. Fadaei-Tirani, I. Zivkovic and M. Mazzanti, *Chem. Sci.*, 2019, **10**, 3543–3555; (*b*) J. Z. Du, D. M. King, L. Chatelain, E. L. Lu, F. Tuna, E. J. L. McInnes, A. J. Wooles, L. Maron and S. T. Liddle, *Chem. Sci.*, 2019, **10**, 3738–3745; (*c*) C. T. Palumbo, L. Barluzzi, R. Scopelliti, I. Zivkovic, A. Fabrizio, C. Corminboeuf and M. Mazzanti, *Chem. Sci.*, 2019, **10**, 8840–8849; (*d*) L. Barluzzi, R. Scopelliti and M. Mazzanti, *J.*

Am. Chem. Soc., 2020, **142**, 19047–19051; (*e*) M. A. Boreen, G. D. Rao, D. G. Villarreal, F. A. Watt, R. D. Britt, S. Hohloch and J. Arnold, *Chem. Commun.*, 2020, **56**, 4535–4538; (*f*) L. Chatelain, E. Louyriac, I. Douair, E. L. Lu, F. Tuna, A. J. Wooles, B. M. Gardner, L. Maron and S. T. Liddle, *Nat. Commun.*, 2020, **11**, 337; (*g*) C. T. Palumbo, R. Scopelliti, I. Zivkovic and M. Mazzanti, *J. Am. Chem. Soc.*, 2020, **142**, 3149–3157; (*h*) M. Yadav, A. J. Metta-Magana and S. Fortier, *Chem. Sci.*, 2020, **11**, 2381–2387; (*i*) L. Barluzzi, F. C. Hsueh, R. Scopelliti, B. E. Atkinson, N. Kaltsoyannis and M. Mazzanti, *Chem. Sci.*, 2021, **12**, 8096–8104; (*j*) J. Z. Du, J. A. Seed, V. E. J. Berryman, N. Kaltsoyannis, R. W. Adams, D. Lee and S. T. Liddle, *Nat. Commun.*, 2021, **12**, 5649.

14 (*a*) W. J. Evans, S. A. Kozimor and J. W. Ziller, *Polyhedron*, 2004, **23**, 2689–2694; (*b*) D. K. Modder, C. T. Palumbo, I. Douair, F. Fadaei-Tirani, L. Maron and M. Mazzanti, *Angew. Chem., Int. Ed. Engl.*, 2021, **60**, 3737–3744.

15 (*a*) B. Vlaisayljevich, P. L. Diaconescu, W. L. Lukens, Jr., L. Gagliardi and C. C. Cummins, *Organometallics*, 2013, **32**, 1341–1352; (*b*) K. R. Meihaus, S. G. Minasian, W. W. Lukens, S. A. Kozimor, D. K. Shuh, T. Tyliszczak and J. R. Long, *J. Am. Chem. Soc.*, 2014, **136**, 6056–6068; (*c*) L. C. J. Pereira, C. Camp, J. T. Coutinho, L. Chatelain, P. Maldivi, M. Almeida and M. Mazzanti, *Inorg. Chem.*, 2014, **53**, 11809–11811.

16 D. R. Kindra and W. J. Evans, *Chem. Rev.*, 2014, **114**, 8865–8882.

17 P. L. Diaconescu, P. L. Arnold, T. A. Baker, D. J. Mindiola and C. C. Cummins, *J. Am. Chem. Soc.*, 2000, **122**, 6108–6109.

18 (*a*) M. D. Fryzuk, T. S. Haddad and S. J. Rettig, *J. Am. Chem. Soc.*, 1990, **112**, 8185–8186; (*b*) J. A. Pool, E. Lobkovsky and P. J. Chirik, *Nature*, 2004, **427**, 527–530; (*c*) Y. Ohki and M. D. Fryzuk, *Angew. Chem., Int. Ed. Engl.*, 2007, **46**, 3180–3183.

19 (*a*) R. D. Sanner, D. M. Duggan, T. C. McKenzie, R. E. Marsh and J. E. Bercaw, *J. Am. Chem. Soc.*, 1976, **98**, 8358–8365; (*b*) W. J. Evans, T. A. Ulibarri and J. W. Ziller, *J. Am. Chem. Soc.*, 1988, **110**, 6877–6879; (*c*) T. E. Hanna, E. Lobkovsky and P. J. Chirik, *J. Am. Chem. Soc.*, 2004, **126**, 14688–14689.

20 J. C. Wedal, J. M. Barlow, J. W. Ziller, J. Y. Yang and W. J. Evans, *Chem. Sci.*, 2021, **12**, 8501–8511.

21 T. Suzuki, K. Fujimoto, Y. Takemoto, Y. Wasada-Tsutsui, T. Ozawa, T. Inomata, M. D. Fryzuk and H. Masuda, *ACS Catal.*, 2018, **8**, 3011–3015.

22 S. Fortier, J. L. Brown, N. Kaltsoyannis, G. Wu and T. W. Hayton, *Inorg. Chem.*, 2012, **51**, 1625–1633.

23 (*a*) J. S. Silvia and C. C. Cummins, *J. Am. Chem. Soc.*, 2009, **131**, 446–447; (*b*) B. Askevold, J. T. Nieto, S. Tussupbayev, M. Diefenbach, E. Herdtweck, M. C. Holthausen and S. Schneider, *Nat. Chem.*, 2011, **3**, 532–537; (*c*) P. A. Cleaves, D. M. King, C. E. Kefalidis, L. Maron, F. Tuna, E. J. L. McInnes, J. McMaster, W. Lewis, A. J. Blake and S. T. Liddle, *Angew. Chem., Int. Ed. Engl.*, 2014, **53**, 10412–10415; (*d*) J. A. Buss, C. Cheng and T. Agapie, *Angew. Chem., Int. Ed. Engl.*, 2018, **57**, 9670–9674.

24 M. Falcone, C. E. Kefalidis, R. Scopelliti, L. Maron and M. Mazzanti, *Angew. Chem., Int. Ed. Engl.*, 2016, **55**, 12290–12294.